Kinetic understanding of nitrogen supply condition on biosynthesis of polyhydroxyalkanoate from benzoate by *Pseudomonas putida* KT2440

Zhangyang Xu[1], Xiaolu Li[1], Naijia Hao[2], Chunmei Pan[1], Luis de la torre[3], Aftab Ahamed[1], John H. Miller[3], Arthur J. Ragauskas[2,4,5], Joshua Yuan[6], Bin Yang[1*]

1. Department of Biological Systems Engineering, Washington State University, Richland, WA, 99354, USA.

2. Department of Chemical and Biomolecular Engineering, University of Tennessee, Knoxville, Tennessee, 37996, USA.

3. School of Engineering and Applied Sciences, Washington State University, Richland, WA, 99354, USA.

4. Biosciences Division, Oak Ridge National Laboratory, Oak Ridge, Tennessee, 37831, USA.

5. Department of Forestry, Wildlife, and Fisheries, Center for Renewable Carbon, University of Tennessee Institute of Agriculture, Knoxville, Tennessee, 37996, USA.

6. Synthetic and Systems Biology Innovation Hub, Department of Plant Pathology and Microbiology, Texas A&M University, College Station, 77843, USA

*Corresponding Author:

Dr. Bin Yang, Department of Biological Systems Engineering, Washington State University, 2710 Crimson Way, Richland, Washington, 99354, USA.

E-mail address: bin.yang@wsu.edu

Abstract

Nitrogen supply is critical to the synthesis of intracellular PHA in various bacteria. However, the specific role of the nitrogen in synthesizing PHA from benzoate, a lignin model compound use for the study of bacteria catabolism of aromatics, is still not clear. In this study, two culture conditions were maintained for *P. putida* KT2440 to produce PHA using benzoate as a carbon source. Under nitrogen limited and surplus conditions, the accumulation of PHA was to 37.3% and 0.25% of cell dry weight, respectively. A model fit to the kinetics of biomass growth and PHA accumulation showed good agreement with data. GC-MS and NMR showed that PHA contained six hydroxyl fatty acid monomers in nitrogen-limited condition, while two monomers were identified under surplus nitrogen conditions. The average molecular weight of PHA increased after the nitrogen source was exhausted. These results provide a promising strategy for optimization of lignin to PHA yields.

Keywords: Polyhydroxyalkanoates; *Pseudomonas putida* KT2440; Benzoate; Nitrogen; Kinetic modeling.

1. Introduction

Lignin is one of the three biopolymers of plant biomass and the second most abundant organic polymer on earth and thus plays a vital role in the carbon cycle (Austin and Ballaré, 2010). Aerobic fungi and some bacteria degrade lignin into humus and aromatic compounds which both increase soil fertility. Aromatic compounds are abundant in soil and comprise about one-quarter of the earth's biomass composition. Recently, the use of aromatic compounds as feedstock for the production of a series of bioproducts, including fuels and chemicals, has attracted much attention (Xu et al., 2018). *P. putida* has been studied extensively due to its robust, aromatic degradation system (Tsipa et al., 2017). Moreover, it contains type II phaC polymerases, which can synthesize medium chain length PHA ranging from C_6 - C_{14} (Cheema et al., 2012). These characteristics made *P. putida* KT2440 an ideal strain for converting aromatic compounds into PHA.

PHA is a family of polyesters that can be utilized as carbon storage products by various kinds of bacteria. PHA is the promising renewable bioplastic polymers that are expected to replace traditional chemical synthetic plastic due to their biodegradability and biocompatibility (Imre and Pukánszky, 2013). Unlike synthetic plastics, PHA can be degraded within a few weeks when buried in soil (Dharmalingam et al., 2016). Also, the versatility of PHA, their non-toxic degradation products and lack of carcinogenic effects have enabled their use as *in vivo* implants for medical applications such as sutures, adhesion barriers, and valves to guide tissue repair (Ali and Jamil, 2016). The commercialization of PHA is hindered by its high

cost of production, which in turn is mainly due to having low carbon conversion efficiency (Chen and Jiang, 2017). Efforts have been made to overcome the cost obstacle, including using alternate carbon sources (Chan et al., 2006), genetically manipulating PHA-synthesizing pathways (Cai et al., 2009), and regulating the fermentation processes (Kourmentza et al., 2017). The biosynthesis of PHA is usually caused by certain conditions with deficiencies in nutrients such as phosphorus, nitrogen, and/or oxygen, coupled with a sufficient carbon source supply (Jin et al., 2013). Therefore, many studies chose a nitrogen-limited strategy to increase the yield of PHA (Goh et al., 2014; Shahid et al., 2013; Titz et al., 2012). In *Pseudomonas sp.*, nitrogen metabolism is mainly regulated by a cascade of regulatory proteins, namely, the NTR system. The final response regulator in the NTR system is the NtrC regulator protein. In nitrogen-limited conditions, NtrC is activated by phosphorylation, preventing the remaining carbon source from entering the TCA cycle and stimulating the conversion of excess carbon into storage polymers, including PHA and glycogen (Hervás et al., 2009; Yeom et al., 2010). Therefore, understanding the benzoate-to-PHA process in nitrogen limited/surplus conditions will enable researchers to predict and optimize the PHA yield through a combination of real-time experiments and modeling.

Due to the complex and heterogeneous structure of lignin, analyzing lignin derivatives would simplify the process and help decipher the lignin-to-PHA route. Most of the previous studies mainly focused on PHA production from lignin derivatives including vanillin/vanillic acid (Tomizawa et al., 2014; Wang et al., 2018),

ferulic acid (Linger et al., 2014; Liu et al., 2017) and *p*-coumaric acid (Linger et al., 2014; Liu et al., 2017). Also, some previous publication reported the benzoate-to-PHA route in other strains such as *Desulfococcus multivorans* (Hai et al., 2004) or *Pandoraea sp.* (Kumar et al., 2018), indicating that PHA synthesize was activated by stress response and PHA synthase up-regulation. In a previous *in silica* model, Nogales et al. (2008) predicted the benzoate-to-PHA route through the β-ketoadipate pathway in *P. putida* KT2440. However, the benzoate-to-PHA route was not experimentally analyzed in *P. putida* KT2440, which is a knowledge gap in the current lignin-to-PHA puzzle. Besides, few previous reports focus on the specific role of the nitrogen source in synthesizing PHA from benzoate, one important lignin derivative, in *P. putida* and its kinetic model.

In this study, the bacterial strain *P. putida* KT2440 synthesizes PHA using benzoate as the sole carbon source with either a limited or a surplus nitrogen supply. The production of different PHA monomers was investigated under two different nitrogen supply conditions. In addition, the analysis of the benzoate degradation and the PHA synthesis processes was carried out through kinetic modeling.

2. Materials and Methods

2.1 Microorganism and medium

The bacterial strain *Pseudomonas putida* KT2440 was purchased from American Type Culture Collection (ATCC 47054) and stored in 25% glycerol solution at – 80°C for further use. To obtain a single colony, defrosted bacterial strain *P. putida* was streaked onto Luria-Bertani (Miller's LB agar, CatLog #L3147, Sigma) agar plates

and incubated at 28°C for 24 hours. An isolated single colony was picked from the plate and inoculated into a 500 mL shake flask containing 200 mL of Luria-Bertani liquid medium (Miller's LB Broth, CatLog #L3522, Sigma) containing 10 $g \cdot L^{-1}$ Tryptone, 10 $g \cdot L^{-1}$ NaCl, 5 $g \cdot L^{-1}$ Yeast Extract and incubate in a shaker at 180 rpm and set to 28°C for 24 hours. The bacterial cells were harvested by centrifugation at 8014 × g (8000 rpm) for 5 min using Eppendorf 5804 centrifuge, washed twice with 0.9% sodium chloride solution, and re-suspended in 20 mL 0.9% sodium chloride solution as the inoculation seed material. A calculated volume of seed material (around 12 mg of cells) was inoculated into 250 mL Erlenmeyer flasks with 100 mL of pre-prepared M9 mineral salts medium and cultivated in a shaking incubator (Jeio Tech ISF-7100, Korea) at 180 rpm and set to 28 °C for 24 hours. The composition of M9 mineral medium was as follows: 6 $g \cdot L^{-1}$ Na_2HPO_4, 3 $g \cdot L^{-1}$ KH_2PO_4, 0.5 $g \cdot L^{-1}$ NaCl, 0.12 $g \cdot L^{-1}$ $MgSO_4$ and 1 $mL \cdot L^{-1}$ trace element solution: 3 µM $(NH_4)_6Mo_7O_{24} \cdot 4H_2O$, 0.4mM H_3BO_3, 30 µM $CoCl_2 \cdot 6H_2O$, 10 µM $CuSO_4 \cdot 5H_2O$, 80µM $MnCl_2 \cdot 4H_2O$, 10µM $ZnSO_4 \cdot 7H_2O$, 1mM $FeSO_4 \cdot 7H_2O$ (Lin et al., 2016; Sambrook, 2001). The M9 mineral medium was supplemented with sodium benzoate (1 $g \cdot L^{-1}$) along with two different concentrations of NH_4Cl separately to maintain the nitrogen surplus condition (1 $g \cdot L^{-1}$) and nitrogen limited condition (50 $mg \cdot L^{-1}$). Every treatment was a set three replicates with a total of 36 flasks.

Three flasks from each condition sacrificed for harvesting cells every 2 hours. The harvested cells were centrifuged at 8014 × g (8000 rpm) for 5 min using Eppendorf 5804 centrifuge, washed twice with 5 mL of 0.9% sodium chloride

solution, and freeze-dried to record the cell weight.

2.2 GC-MS analysis for PHA polymer isolation and characterization.

The freeze-dried cells (around 40 mg) were ground, weighed, and extracted with 7 mL chloroform at 60°C in a shaking incubator set to 150 rpm for 12 hours. Each extractive was filtered into separate reaction tubes (KIMAX reusable tubes with a PTFE-faced rubber-lined screw cap, catalog no. #14-930-10B) using a 0.2 μm nylon membrane filter and concentrated to 1 mL by passing nitrogen for around 20 min. 10 mL methanol was added to precipitate the polymer at 4°C and leave it for 3 days. The mixture in methanol was centrifuged at 1127 × g (3000 rpm) for 5 min, separating the organic solution for disposal as chemical waste. The residue was carefully evaporated with nitrogen flow for 5 min. Finally, the PHA polymers were weighted and subjected to further composition analysis.

The PHA monomer-composition analysis was modified by considering several existing methods (Lin et al., 2016; Salvachua et al., 2015; Shen et al., 2009). To be specific, each PHA polymers produced from different samples were placed in separate close-tightened reaction tubes for further analysis. Notably, the empty reaction tubes should be pre-tested at 100°C for 4 hours with 2 mL methanol containing 15% (v/v) sulfuric acid before methanolysis to avoid liquid loss during the heating process. Pairing the lid and tube with no liquid loss after the pre-test experiment was also suggested. Methanolysis was carried out by adding 2 mL methanol containing 15% (v/v) sulfuric acid with PHA polymers and incubating it at 100°C in a conventional oven (BINDER) for 4h. After cooling, 2 mL dichloromethane was added and vortexed

for 1 minute to extract the ester component, then 1 mL Milli-Q water was added to force the organic-phase layering and 2 mL of the bottom organic phase containing methyl ester was transferred into a glass vial, then 0.20 g of calcium carbonate to neutralize the solution were added and filtered with 0.2 μm nylon membrane into the GC vials for GC-MS analysis.

GC-MS analysis was performed using Agilent GC-MS system (7890A GC-system with 5975C inert XL E1/C1 MSD model # G3174A, Agilent Technologies, Wilmington, DE, USA) equipped with DB-5 capillary column (30 m × 0.25 mm × 0.25 μm). The CTC analytics CombiPAL robotic arm (G6500-CTC-LHS2.PAL system-CH001210757, CTC Analytics AG, Zwingen, Switzerland) was connected to GC-MS for auto sampling system (Ahring et al., 2015). The samples were analyzed in splitless mode (injection volume 1μL) using helium as the carrier gas at a flow rate of 1.2 $mL \cdot min^{-1}$. Oven temperature was programmed at an initial temperature of 40 °C for 5 min and subsequently raised at the rate of 10 $°C \cdot min^{-1}$ to 280 °C and held for 5 min. The solvent delay was set at 4.3 min. MS detector using electron impact (EI) ionization at 70 eV was operated in full scans. The mass spectra were generated by scanning ions of m/z 25 to m/z 1000. PHA monomers were initially identified through library comparison using the National Institute of Standards and Technology (NIST) database. The commercial-standard target compounds were purchased from Sigma-Aldrich (SUPELCO 37-component FAME mix in dichloromethane, Catalog #CRM47885). Moreover, one blank dichloromethane vial was also analyzed prior to the analysis of all samples and the values obtained from the blank were subtracted

from the standards and samples (Ahamed and Ahring, 2011).

2.3 NMR analysis

^{1}H and ^{13}C NMR spectra were recorded on a Varian 500 MHz spectrometer. 6-12 mg of PHA was dissolved in 0.5 mL $CDCl_3$ for ^{1}H and ^{13}C NMR analysis. The acquisition parameters were set as follows: 20 °C, pulse angle of 90°, relaxation delay of 5.0 s (for ^{1}H) and 12.0 s (for ^{13}C), scan number of 16 (for ^{1}H) and 6000 (for ^{13}C). The signal from chloroform $\delta_{C/H}$ = 77.2/7.26 ppm was used for chemical shift calibration. Two-dimensional ^{1}H-correlation spectroscopy (2D ^{1}H-COSY) and heteronuclear multiple bond correlation (HMBC) were performed on a Bruker 500 MHz spectrometer. ^{1}H-COSY employed a standard Bruker sequence "cosydfqf" with a scan number of 32 and an increment delay of 200 μsec. HMBC employed a standard Bruker sequence "hmbccgpndqf" with a scan number of 96 and an increment delay of 36 μsec. All the NMR spectra were analyzed with the software Mestrenova (version of 11.0.2) (Muangwong et al., 2016).

2.4 GPC analysis

The number-average molecular weight (Mn) and weight average molecular weight (Mw) of PHA were determined by gel permeation chromatography (GPC). These two types of molecular weight express the average molecular weight in number average and weight average respectively. Prior to GPC analysis, the extracted PHA film (dried) were dissolved in tetrahydrofuran with a concentration of 1 $mg \cdot mL^{-1}$ for 24 h, then filtered through a 0.45 μm filter, and collected in a 2 mL vial (Gumel et al., 2012). The molecular weight distributions of PHA was then analyzed by an Agilent

GPC SECurity 1200 system equipped with Waters Styragel columns (HR0.5, HR2, HR4, HR6) and an Agilent refractive index (RI) detector. THF was used as the mobile phase and the flow rate was set to 1 $mg \cdot mL^{-1}$. The sample injection volume was set to 20 µL. A calibration curve was built using polystyrene standards ranging from 4 x 10^3 $g \cdot mol^{-1}$ to 2 x 10^6 $g \cdot mol^{-1}$. The Mn and Mw results of the PHA were calculated against this calibration curve.

2.5 Determination of Benzoate utilization

1 mL supernatant samples from cell cultures were filtered through a 0.22 µm nylon filter. Then, the determination of the benzoate concentration in M9 culture media was analyzed every two hours in the growth curve of *P. putida* KT2440 by HPLC with a photodiode array detector (Dionex ultimate 3000 model) using an Aminex HPX-87H column programmed at 65 °C and 4M sulfuric acid eluent at a flow rate of 0.6 $mL \cdot min^{-1}$ (Vardon et al., 2016).

2.6 Nitrogen determination assay

The nitrogen concentration in the medium was measured using the method described by Amara et al. (Amara et al., 2016). The supernatant samples were diluted 1000-fold to 10 mL using Milli-Q water and the following reagents, including 0.4 mL 10% phenol (w/v in ethanol), 0.4 mL 0.5 % nitroprusside solution and 1 mL 20% mixed solution (w/v) of trisodium citrate and sodium hypochlorite (Trisodium citrate with 1% sodium hydroxide mixed with 5% sodium hypochlorite at ratio 4:1 (v/v)), were added. All the samples were incubated in a water bath at 37°C for 2h and the absorbance of each sample was measured at 630nm using UV spectrophotometer

(Jenway, 6405 UV/Vis spectrophotometer).

2.7 Kinetic Modeling

A kinetic model was developed to describe the PHA accumulation in *P. putida* KT2440 grown on benzoate as the carbon source in excess (1 $g \cdot L^{-1}$) and deficient (50 $mg \cdot L^{-1}$) nitrogen conditions. The model, a modified version of a kinetic model developed by Economou et al., (2011), predicted that the concentration of PHA would be constant at the beginning, but that it would then increase after the exhaustion of the nitrogen in the presence of benzoate as a carbon source. In general, the basic assumptions of the model are that: 1) Bacterial culturing took place in a shake-flask incubator for batch fermentation. 2) Bacterial growth depended on benzoate and nitrogen sources. 3) The cumulative amount of PHA started small and increased when nitrogen limitation occurred with excess benzoate as a carbon source in the culture media. 4) Benzoate was used for both biomass growth and PHA synthesis. 5) Nitrogen was consumed during PHA-free biomass synthesis. 6) The accumulated PHA was not used for PHA-free biomass synthesis when carbon limitation takes place. 7) PHA production was not inhibited by a high concentration of benzoate under our experimental conditions. The last two assumptions allowed us to use a simplified version of the model (Economou et al., 2011) with fewer parameters (see equations (1) – (6)).

The balance equation for PHA-free biomass in a batch reactor was

$$\frac{dX}{dt} = \mu_{SN} X \tag{1}$$

Where X was the PHA-free biomass concentration ($g \cdot L^{-1}$), and μ_{SN} was the specific growth rate on benzoate and nitrogen (h^{-1}).

The balance equation for accumulated PHA was:

$$\frac{dP}{dt} = q_p X \tag{2}$$

Where P was the concentration of PHA ($g \cdot L^{-1}$), q_p was the specific accumulation rate of lipids in the biomass ($g_{PHA} \cdot g_{PHA\text{-free biomass}}^{-1}$ h).

The balance equation for the benzoate was:

$$-\frac{dS}{dt} = \left(\mu_{SN}\frac{1}{Y_{X/S}} + q_p\frac{1}{Y_{p/S}}\right)X \tag{3}$$

Where S was the concentration of benzoate ($g \cdot L^{-1}$), $Y_{X/S}$ was the yield coefficient for PHA-free biomass production with respect to benzoate ($g_{PHA\text{-free biomass}} \cdot g_{benzoate}^{-1}$), and $Y_{p/S}$ was the yield coefficient for PHA production with respect to benzoate ($g_{PHA} \cdot g_{benzoate}^{-1}$).

The equation for nitrogen consumption for the synthesis of PHA-free biomass was:

$$-\frac{dN}{dt} = \mu_{SN}\frac{1}{Y_{X/N}}X \tag{4}$$

Where N was the nitrogen concentration ($g \cdot L^{-1}$) and $Y_{X/N}$ was the yield coefficient for PHA-free biomass production with respect to nitrogen ($g_{PHA\text{-free biomass}} \cdot g_{nitrogen}^{-1}$).

The specific growth rate on benzoate and nitrogen (μ_{SN}) was assumed to be described by a type of double-substrate limitation according to Andrews' equation:

$$\mu_{SN}(S,N) = \mu_{SNmax}\frac{S}{K_S + S}\frac{N}{K_N + N} \quad (5)$$

Where μ_{SNmax} was the maximum specific growth rate (h^{-1}), K_S and K_N are saturation constants ($g \cdot L^{-1}$).

The specific accumulation rate of PHA in the biomass (q_p) described by Andrews' model for dependence on benzoate concentration:

$$q_p(S,N) = q_{pmax}\frac{S}{K_{PS} + Sk_2 + N}\frac{k_2}{K_{PS} + Sk_2 + N} \quad (6)$$

q_{pmax} was the maximum specific accumulation rate ($g_{PHA} \cdot g_{PHA\text{-free biomass}}^{-1}$ h), K_{PS} was the saturation constant ($g \cdot L^{-1}$), and k_2 was a constant ($g \cdot L^{-1}$) that inhibits PHA production under surplus nitrogen conditions.

3. Results and Discussion

3.1 Determination of cell growth and PHA accumulation.

P. putida KT2440 was capable of transforming benzoate into several PHA monomers in 24 h while growing on M9 medium with benzoate as carbon source ($1 g \cdot L^{-1}$) and nitrogen source at a concentration of $50 mg \cdot L^{-1}$ (Figure 1a and 1b), whereas the PHA accumulation in 24 h was very limited with benzoate ($1 g \cdot L^{-1}$) and nitrogen at a surplus condition of $1 g \cdot L^{-1}$ (Figure 1c and 1d).

PHA accumulation by *P. putida* KT2440 was monitored with $1 g \cdot L^{-1}$ benzoate and nitrogen at $50 mg \cdot L^{-1}$ (Figure 1a). Biomass accumulation exhibited a four-hour lag phase, increased significantly after six hours, and reached its maximum at 16 hours maintaining this level until 24 hours (around 32 mg cell dry weight). PHA weight was maintained at around 1 mg until the 6-hour mark, started to increase after 8 hours

from the start of the experiment, and reached its maximum at 20 hours. This level was maintained until the 24th hour of fermentation (around 12 mg, 37.3% CDW). The benzoate concentration consistently decreased from the start and was completely exhausted after 14 hours of fermentation. The nitrogen source's concentration also started decreased from the start of the experiment and was exhausted after 6 hours of fermentation. Notably, the PHA weight started to increase when the nitrogen was exhausted and benzoate was still sufficient.

The accumulation of PHA by *Pseudomonas putida* KT2440 was monitored over a 24-h period when 1g·L^{-1} of benzoate was supplied to M9 medium containing the nitrogen source at a concentration of 1g·L^{-1} (Figure 1c). Cell dry weight (CDW) started to increase after a 4-hour lag phase, increased significantly at the start of the 6th hour, and reached its maximum at around 40 mg cell dry weight after 16 hours of fermentation. The PHA weight was consistently maintained at a low amount (around 1 mg, 0.25% CDW) from the beginning to the end of the fermentation process. Benzoate concentration consistently decreased from the very beginning and was exhausted after 14 hours of fermentation. The nitrogen source concentration fluctuated at around 0.8 g·L^{-1} throughout the fermentation process. Notably, the PHA weight did not increase as cell dry weight increased under conditions where nitrogen was in excess.

Nitrogen source has been considered the limiting factor for the PHA synthesis process (Titz et al., 2012). In nitrogen-deprived conditions, *P. putida* mt-2 could convert various carbon sources into PHA (Shahid et al., 2013) and PHA synthesis

started when nitrogen source became the limiting factor (Xi et al., 2000). This is consistent with our results where PHA started to be formed when the nitrogen source became exhausted in the medium. In the previous investigation of the conversion of lignin derivatives to PHA, Tomizawa et al. (2014) screened twelve strains grown on 18 aromatic compounds (Tomizawa et al., 2014). Though *P. putida* 13063, *P. putida* GPo1 and *P. aeruginosa* all could grow on vanillic acid, 4-hydroxybenzoic acid, and 3,4-dihydroxybenzoic acid, PHA accumulation was less than 1 wt% due to the initial high nitrogen source loading (0.5 $g \cdot L^{-1}$). This result is very similar to our finding that PHA did not accumulate when the nitrogen source was abundant in the medium. Pathway map from benzoate to PHA was exhibited in the supplementary material.

3.2 Comparing the PHA monomers in different nitrogen conditions.

PHA monomers exhibited different distributions in nitrogen-limited and nitrogen surplus conditions. The 24th hours of fermentation samples were picked up for showing the PHA monomer difference between nitrogen limited (Figure 1b) and nitrogen surplus (Figure 1d) condition by GC/MS chromatograph. In nitrogen-limited conditions, PHA monomers mainly identified of six monomers, whereas only two monomers were identified in surplus nitrogen conditions (Table 1).

Comparing the composition of the monomers after 24 hours of fermentation, in nitrogen-limited conditions, 3-hydroxyoctanoate and 3-hydroxydecanoate accounted for 51.96% and 28.08% (mol% of PHA, Table 1), respectively. All other monomers individually composed less than 10% (mol% of PHA, Table 1) of all the monomers, whereas in nitrogen-surplus conditions, 3-hydroxydecanoate and 3-

hydroxyhexadecanoate accounted for 58.00% and 42.00% (mol% of PHA, Table 1) of the monomers, respectively. Notably, in nitrogen-limited conditions, all the PHA polymers were synthesized after the nitrogen was exhausted. This indicated that the depletion of the nitrogen source triggered PHA synthesis, which has been addressed in previous reports (Chakraborty et al., 2012; Fu et al., 2015). Moreover, our results indicate that all the monomers started to synthesize at the same time after the nitrogen was depleted.

Six-monomer compositions of the PHA were further confirmed by ^{1}H, COSY and the HMBC NMR analysis of the polymer. The ^{1}H-NMR spectral data of the PHA obtained by cultivating *P. putida* with benzoate in nitrogen-limited and nitrogen-surplus conditions is shown in supplementary material. To further elucidate the structure of the PHA, ^{1}H-^{1}H COSY and HMBC NMR analyses were applied. ^{1}H-^{1}H COSY spectra of the PHA produced from nitrogen-limited conditions were shown in supplementary material. The detailed proton chemical shift assignment was labeled in Figure 2b: 0.86 ppm (a, -CH_3), 1.25 ppm (b, -CH_2 in side chain), 1.58 ppm (c, -CH_2 in side chain), 1.66 ppm (d, -CH_2 adjacent to a C=C), 2.03 ppm (e, -CH_2 adjacent to a C=C), 2.52 ppm (f, -CH_2- next to C=O), 5.16 ppm (g, -CH- next to O), and 7.24 ppm (h, $CHCl_3$) (Watanabe et al., 2015; Levine et al., 2016; Muangwong et al., 2016). Although the proton signals (1.66 ppm, 2.03 ppm) next to the unsaturated carbon double bonds were detected in the COSY spectra, the proportion of the unsaturated chains were extremely limited. The integration results show that protons adjacent to a C=C are only ~1.92% of the saturated proton signals of CH_2. The HMBC spectra

present the information of $^{1}H/^{13}C$ multiple bond coherence. The HMBC spectra of the PHA produced from the nitrogen-limited conditions were presented in supplementary material. The proton/carbon pairs were labeled. The first number in the pair refers to the proton and the second number refers to the carbon. Since no decoupling was applied in the sequence, the single bond coherence (pairs of identical proton/carbon numbers) that existed in the spectra was split by the large single bond couplings (de Waard et al., 1993). The cross-peaks of the pair of the unsaturated carbon and the adjacent proton (usually appears at around 122/2.0 ppm, 135/2.0 ppm, 122/2.4 ppm, 135/2.4 ppm) were not found in HMBC spectra at this zooming level, which suggested that unsaturated carbon contents were limited and that this finding was consistent with the COSY spectra (de Waard et al., 1993). The single and multiple bond coherences of the HMBC spectra of the PHA produced in the nitrogen surplus conditions were also labeled in the spectra.

Previously, it was reported that when *P. putida* A514 was grown on vanillin in nitrogen-limited conditions (Lin et al., 2016), PHA mainly consisted of 3-hydroxyhexanoate, 3-hydroxyoctanoate, 3-hydroxydecanoate, 3-hydroxydodecanoate, and 3-hydroxyhexadecanoate. However, in conditions with surplus nitrogen, only 3-hydroxydecanoate and 3-hydroxyhexadecanoate were observed. The monomer distributions were similar to our results, but the composition of the monomers was different with different aromatics as feedstock (Lin et al., 2016).

3.3 Monitoring the PHA monomers distribution over time.

PHA monomers were monitored in nitrogen-limited conditions and exhibited a

specific triggering effect on PHA synthesis after the nitrogen source was exhausted. At the beginning of fermentation (supplementary material), no obvious PHA monomer peak was identified in the GC-MS spectrum (supplementary material). But immediately after the nitrogen source was exhausted, six PHA monomers were identified (Nitrogen-limited conditions: 8 hours). All six monomers were identified in 12 hours of fermentation. All the peak ratios of PHA monomers were increased until the 24th hour of fermentation (supplementary material). In the ^{1}H-NMR spectrum (supplementary material), all the peaks were identified in the 0th hour of fermentation, which means that all monomers existed at the beginning of fermentation and the peak intensity was maintained at the same level after 8 hours of fermentation, which was consistent with GC-MS results.

3.4 PHA molecular weight over time.

The molecular weight distribution of the PHA was determined by GPC using polystyrene standards for calibration. The results of the weight average molecular weight (Mw), the number average molecular weight (Mn), and the polydispersity (D) of PHA were presented in supplementary material. Figure 2 shows that the Mw trends of the PHA were detected every four hours of fermentation in both nitrogen-limited and nitrogen-surplus conditions. In nitrogen-limited conditions, the PHA produced from 4 hours of fermentation exhibited a Mw of 5.52×10^{4} Da, and 8 hours of fermentation enhanced the Mw of PHA to 1.47×10^{5} Da. After 8 hours of fermentation in nitrogen-limited conditions, the Mw of the PHA was maintained at the same level and no further increase was detected. The PHA produced after 24 hours under

nitrogen-limited conditions exhibited a Mw of 1.18×10^5 Da, Mn of 5.74×10^4 Da, and a polydispersity which was consistent with the PHA molecular weight results reported in published literature (Kourmentza et al., 2018; Levine et al., 2016; Linger et al., 2014). Linger et al. used the same organism, *P. putida* KT2440, to convert lignin-rich stream to middle chain length PHA. The lignin-rich stream-derived PHA had a Mw of 1.24×10^5 Da, Mn of 6.40×10^4 Da, and a D of 1.93, which are similar to the molecular weight distribution of the PHA produced from benzoate in this study (Linger et al., 2014). For conditions with a surplus of nitrogen, the PHA molecular weight was constant until the 24th hour, which is consistent with the PHA yield results that show that no PHA was accumulated during the whole fermentation period. As for the polydispersity index (D) values, the PHA produced from nitrogen limited conditions had a D value ranging from 2.84 to 2.05, which was consistent with the results reported in the literature, which claimed that the step polymerization reactions typically had a D value of around 2.0 (Muangwong et al., 2016). After a fermentation time of 8 hours, the D values of PHAs generated from nitrogen-limited conditions showed a decreasing trend from 2.84 to 2.05, which suggested a narrower molecular weight distribution was obtained after a longer fermentation time in this study. The similar trend for D values was not found under nitrogen-surplus conditions.

3.5 Modeling cell growth and PHA accumulation.

As shown in Figure 1c, the contribution of PHA to biomass under surplus nitrogen conditions is very small; hence, the biomass data can be interpreted as PHA-free biomass. Figure 1a shows that under nitrogen-limited conditions, the dynamics of

biomass production had two components: an early component when the yield of PHA was low and a later component that received a substantial contribution from PHA synthesis. To obtain PHA-free biomass data for model-fitting under nitrogen-limited conditions, we subtracted the PHA yield data from the total biomass data. Since both types of data contain experimental uncertainty, the PHA-free biomass data obtained with this approach has more scatter than the data from which it was derived and makes the fit to PHA-free biomass under limited nitrogen more uncertain than is the case under surplus nitrogen.

The fit to the PHA yield under limited nitrogen (Figure 3a) was added to the fit to PHA-free biomass under limited nitrogen to obtain the comparison of the model to data on total biomass shown in Figure 4a. For all the results shown in Figure 4, fitting began at 2 hours because, as shown in Figures 1a and 1c, biomass decreased between 0 and 2 hours under both surplus and limited nitrogen conditions. We interpret this decrease as the result of the adjustment of the cell culture to conditions in the fermenter.

Due to the simpler dynamics, the agreement between data and fitted model is better for surplus nitrogen conditions, shown in Figures 3b, than for nitrogen-limited conditions, shown in Figures 3a. Note in particular the good fit to the decreasing concentration of benzoate in the medium. Both the model and data agree that after 14 hours, this carbon source was exhausted, which is consistent with the observed saturation of biomass production under surplus nitrogen conditions after 14 hours.

The largest deviation of the model from the data is in the kinetics of nitrogen

under conditions of limited nitrogen, where the model predicts a significantly higher concentration of nitrogen than is observed in the medium between the first 6 and 8 hours of fermentation. To fit the significant increase in PHA-free biomass observed between 6 and 10 hours as well as the observation that, within experimental error, there is no increase in PHA yield in the first 10 hours, the model requires a rate of nitrogen decrease that is slower than that observed experimentally. These results suggest the presence of a source of nitrogen other than what is being measured in the growth medium.

Another unusual aspect of the kinetics of nitrogen in the medium is the significant decrease (~20%) between 0 and 2 hours. In the same period, the benzoate concentration decreases by only about 2% and there is no increase in biomass. Similar kinetic relationships are seen in the first 2 hours under both limited and surplus nitrogen conditions (see Figures 1a and 1c) even though the initial concentrations of nitrogen differ by a factor of 20. We conclude from these results that the kinetics observed for the nitrogen concentration in the medium are not related to biomass production in the way that is expected from the model being used to fit the data and that additional factors not in the model are influencing these kinetics.

Estimates of a subset of the parameters in the model of Economou et al. (2011) (see section 2.7) were obtained by fitting the model to the data acquired under limited and surplus nitrogen conditions were listed in supplementary material. Since q_{pmax} is zero under conditions of excess nitrogen, the model predicts a constant level of PHA as seen in Figure (1c) and the parameters $Y_{X/N}$, K_{PS} and k_2 cannot be determined

in this case (see Eq. 6 in section 2.7).

4. Conclusions

This study investigated the effects of the nitrogen source on benzoate-to-PHA convention by *P. putida* KT2440. By analyzing the PHA synthesis process with GC-MS, NMR, GPC, and kinetic modeling, two distinct PHA synthesis patterns were elucidated. Exhaustion of nitrogen source in the medium acted as the trigger for accumulation of mcl-PHA monomers. A kinetic model agreed with data on production of biomass and PHA, and consumption of benzoate but suggested the presence of more nitrogen than observed in the medium. Our results provide better understanding of the benzoate-to-PHA process, which may lead to high yield of PHA from biomass-derived lignin.

5. Competing financial interests

The authors declare no competing financial interests.

Acknowledgments

This work is supported by the U.S. Department of Energy (DOE), the Office of Energy Efficiency & Renewable Energy (EERE) Awards (DE-EE0007104 and DE-EE0006112), and the Bioproducts, Science and Engineering Laboratory, Department of Biological Systems Engineering at Washington State University. This work was performed in part at the William R. Wiley Environmental Molecular Science Laboratory (EMSL), a national scientific user facility sponsored by the U.S. Department of Energy's Office of Biological and Environmental Research and located at the Pacific Northwest National Laboratory, operated for the Department of Energy

by Battelle. Ms. X. Li and Dr. C. Pan were partially supported by CSC Scholarship for Overseas Studies.

Appendix A. Supplementary data

Supplementary data associated with this article can be found, in the online version of this paper.

References

1. Ahamed, A., Ahring, B.K. 2011. Production of hydrocarbon compounds by endophytic fungi *Gliocladium* species grown on cellulose. Bioresour Technol. 102(20), 9718-9722.
2. Ahring, B.K., Biswas, R., Ahamed, A., Teller, P.J., Uellendahl, H. 2015. Making lignin accessible for anaerobic digestion by wet-explosion pretreatment. Bioresour Technol. 175, 182-188.
3. Ali, I., Jamil, N. 2016. Polyhydroxyalkanoates: Current applications in the medical field. Front. Biol. 11(1), 19-27.
4. Amara, S., Seghezzi, N., Otani, H., Diaz-Salazar, C., Liu, J., Eltis, L.D. 2016. Characterization of key triacylglycerol biosynthesis processes in *rhodococci*. Sci Rep. 6, 24985.
5. Austin, A.T., Ballaré, C.L. 2010. Dual role of lignin in plant litter decomposition in terrestrial ecosystems. Proc Natl Acad Sci USA. 107(10), 4618-4622.
6. Cai, L., Yuan, M.Q., Liu, F., Jian, J., Chen, G.Q. 2009. Enhanced production of medium-chain-length polyhydroxyalkanoates (PHA) by PHA depolymerase knockout mutant of *Pseudomonas putida* KT2442. Bioresour Technol. 100(7),

2265-2270.

7. Chakraborty, P., Muthukumarappan, K., Gibbons, W.R. 2012. PHA Productivity and Yield of *Ralstonia eutropha* When Intermittently or Continuously Fed a Mixture of Short Chain Fatty Acids. J. Biomed. Biotechnol. 2012, 506153.
8. Chan, P.L., Yu, V., Wai, L., Yu, H.-F. 2006. Production of medium-chain-length polyhydroxyalkanoates by *pseudomonas aeruginosa* with fatty acids and alternative carbon sources. Appl Biochem Biotechnol. 132(1), 933-941.
9. Cheema, S., Bassas-Galia, M., Sarma, P.M., Lal, B., Arias, S. 2012. Exploiting metagenomic diversity for novel polyhydroxyalkanoate synthases: Production of a terpolymer poly(3-hydroxybutyrate-co-3-hydroxyhexanoate-co-3-hydroxyoctano-ate) with a recombinant *Pseudomonas putida* strain. Bioresour Technol. 103(1), 322-328.
10. Chen, G.Q., Jiang, X.R. 2017. Engineering bacteria for enhanced polyhydroxyalkanoates (PHA) biosynthesis. Syst. Synth. Biol. 2(3), 192-197.
11. de Waard, P., van der Wal, H., Huijberts, G.N., Eggink, G. 1993. Heteronuclear NMR analysis of unsaturated fatty acids in poly(3-hydroxyalkanoates). Study of beta-oxidation in *Pseudomonas putida*. J. Biol. Chem. 268(1), 315-319.
12. Dharmalingam, S., Hayes, D.G., Wadsworth, L.C., Dunlap, R.N. 2016. Analysis of the time course of degradation for fully biobased nonwoven agricultural mulches in compost-enriched soil. Text Res J. 86(13), 1343-1355.
13. Economou, C.N., Aggelis, G., Pavlou, S., Vayenas, D.V. 2011. Modeling of single-cell oil production under nitrogen-limited and substrate inhibition

conditions. Biotechnol Bioeng. 108(5), 1049-1055.

14. Fu, J., Sharma, P., Spicer, V., Krokhin, O.V., Zhang, X., Fristensky, B., Cicek, N., Sparling, R., Levin, D.B. 2015. Quantitative 'Omics Analyses of Medium Chain Length Polyhydroxyalkanaote Metabolism in *Pseudomonas putida* LS46 Cultured with Waste Glycerol and Waste Fatty Acids. PLoS ONE, 10(11), e0142322.
15. Goh, L.K., Purama, R.K., Sudesh, K. 2014. Enhancement of Stress Tolerance in the Polyhydroxyalkanoate Producers without Mobilization of the Accumulated Granules. Appl Biochem Biotechnol. 172(3), 1585-1598.
16. Gumel, A.M., Annuar, M.S.M., Heidelberg, T. 2012. Biosynthesis and Characterization of Polyhydroxyalkanoates Copolymers Produced by *Pseudomonas putida* Bet001 Isolated from Palm Oil Mill Effluent. PLOS ONE, 7(9), e45214.
17. Hai, T., Lange, D., Rabus, R., Steinbüchel, A. 2004. Polyhydroxyalkanoate (PHA) Accumulation in Sulfate-Reducing Bacteria and Identification of a Class III PHA Synthase (PhaEC) in *Desulfococcus multivorans*. Appl Environ Microbiol. 70(8), 4440-4448.
18. Hervás, A.B., Canosa, I., Little, R., Dixon, R., Santero, E. 2009. NtrC-Dependent Regulatory Network for Nitrogen Assimilation in *Pseudomonas putida*. J Bacteriol. 191(19), 6123-6135.
19. Imre, B., Pukánszky, B. 2013. Compatibilization in bio-based and biodegradable polymer blends. Eur Polym J. 49(6), 1215-1233.
20. Jin, Y.X., Shi, L.H., Kawata, Y. 2013. Metabolomics-based component profiling

of *Halomonas* sp. KM-1 during different growth phases in poly(3-hydroxybutyrate) production. Bioresour Technol. 140, 73-79.

21. Kourmentza, C., Costa, J., Azevedo, Z., Servin, C., Grandfils, C., De Freitas, V., Reis, M.A.M. 2018. Burkholderia thailandensis as a microbial cell factory for the bioconversion of used cooking oil to polyhydroxyalkanoates and rhamnolipids. Bioresour Technol. 247, 829-837.
22. Kourmentza, C., Placido, J., Venetsaneas, N., Burniol-Figols, A., Varrone, C., Gavala, H.N., Reis, M.A.M. 2017. Recent Advances and Challenges towards Sustainable Polyhydroxyalkanoate (PHA) Production. Bioengin. (Basel) 4(2), 55.
23. Kumar, M., Verma, S., Gazara, R.K., Kumar, M., Pandey, A., Verma, P.K., Thakur, I.S. 2018. Genomic and proteomic analysis of lignin degrading and polyhydroxyalkanoate accumulating β-proteobacterium *Pandoraea* sp. ISTKB. Biotechnol Biofuels. 11(1), 154.
24. Levine, A.C., Heberlig, G.W., Nomura, C.T. 2016. Use of thiol-ene click chemistry to modify mechanical and thermal properties of polyhydroxyalkanoates (PHAs). Int J Biol Macromol. 83, 358-365.
25. Lin, L., Cheng, Y., Pu, Y., Sun, S., Li, X., Jin, M., Pierson, E.A., Gross, D.C., Dale, B.E., Dai, S.Y., Ragauskas, A.J., Yuan, J.S. 2016. Systems biology-guided biodesign of consolidated lignin conversion. Green Chem. 18(20), 5536-5547.
26. Linger, J.G., Vardon, D.R., Guarnieri, M.T., Karp, E.M., Hunsinger, G.B., Franden, M.A., Johnson, C.W., Chupka, G., Strathmann, T.J., Pienkos, P.T., Beckham, G.T. 2014. Lignin valorization through integrated biological funneling

and chemical catalysis. Proc Natl Acad Sci USA. 111(33), 12013-8.

27. Liu, Z.-H., Olson, M.L., Shinde, S., Wang, X., Hao, N., Yoo, C.G., Bhagia, S., Dunlap, J.R., Pu, Y., Kao, K.C., Ragauskas, A.J., Jin, M., Yuan, J.S. 2017. Synergistic maximization of the carbohydrate output and lignin processability by combinatorial pretreatment. Green Chem. 19(20), 4939-4955.

28. Muangwong, A., Boontip, T., Pachimsawat, J., Napathorn, S.C. 2016. Medium chain length polyhydroxyalkanoates consisting primarily of unsaturated 3-hydroxy-5-cis-dodecanoate synthesized by newly isolated bacteria using crude glycerol. Microb Cell Fact. 15, 55.

29. Nogales, J., Palsson, B.Ø., Thiele, I. 2008. A genome-scale metabolic reconstruction of *Pseudomonas putida* KT2440: i JN746 as a cell factory. BMC Syst. Biol. 2(1), 79.

30. Salvachua, D., Karp, E.M., Nimlos, C.T., Vardon, D.R., Beckham, G.T. 2015. Towards lignin consolidated bioprocessing: simultaneous lignin depolymerization and product generation by bacteria. Green Chem. 17(11), 4951-4967.

31. Sambrook, J. 2001. Molecular cloning: a laboratory manual. Third edition. Cold Spring Harbor, New York.

32. Shahid, S., Mosrati, R., Ledauphin, J., Amiel, C., Fontaine, P., Gaillard, J.-L., Corroler, D. 2013. Impact of carbon source and variable nitrogen conditions on bacterial biosynthesis of polyhydroxyalkanoates: Evidence of an atypical metabolism in *Bacillus megaterium* DSM 509. J Biosci Bioeng. 116(3), 302-308.

33. Shen, X.W., Yang, Y., Jian, J., Wu, Q., Chen, G.-Q. 2009. Production and

characterization of homopolymer poly(3-hydroxyvalerate) (PHV) accumulated by wild type and recombinant *Aeromonas hydrophila* strain 4AK4. Bioresour Technol. 100(18), 4296-4299.

34. Titz, M., Kettl, K.H., Shahzad, K., Koller, M., Schnitzer, H., Narodoslawsky, M. 2012. Process optimization for efficient biomediated PHA production from animal-based waste streams. Clean Technol Environ Policy. 14(3), 495-503.

35. Tomizawa, S., Chuah, J.-A., Matsumoto, K., Doi, Y., Numata, K. 2014. Understanding the Limitations in the Biosynthesis of Polyhydroxyalkanoate (PHA) from Lignin Derivatives. ACS Sustain Chem Eng. 2(5), 1106-1113.

36. Tsipa, A., Koutinas, M., Vernardis, S.I., Mantalaris, A. 2017. The impact of succinate trace on pWW0 and ortho-cleavage pathway transcription in *Pseudomonas putida* mt-2 during toluene biodegradation. Bioresour Technol. 234, 397-405.

37. Vardon, D.R., Rorrer, N.A., Salvachua, D., Settle, A.E., Johnson, C.W., Menart, M.J., Cleveland, N.S., Ciesielski, P.N., Steirer, K.X., Dorgan, J.R., Beckham, G.T. 2016. cis,cis-Muconic acid: separation and catalysis to bio-adipic acid for nylon-6,6 polymerization. Green Chem. 18(11), 3397-3413.

38. Wang, X., Lin, L., Dong, J., Ling, J., Wang, W., Wang, H., Zhang, Z., Yu, X. 2018. Simultaneous Improvements of *Pseudomonas* Cell Growth and Polyhydroxyalkanoate Production from a Lignin Derivative for Lignin-Consolidated Bioprocessing. Appl. Environ. Microbiol. 84(18), e01469-18.

39. Watanabe, Y., Ishizuka, K., Furutate, S., Abe, H., Tsuge, T. 2015. Biosynthesis

and characterization of novel poly(3-hydroxybutyrate-co-3-hydroxy-2-methylbutyrate): thermal behavior associated with α-carbon methylation. RSC Adv. 5(72), 58679-58685.

40. Xi, J., Wu, Q., Yan, Y., Zhang, Z., Yu, P.H., Cheung, M.K., Zhang, R., Chen, G.Q. 2000. Hyperproduction of polyesters consisting of medium-chain-length hydroxyalkanoate monomers by strain *Pseudomonas stutzeri* 1317. Antonie Van Leeuwenhoek. 78(1), 43-9.

41. Xu, R., Zhang, K., Liu, P., Han, H., Zhao, S., Kakade, A., Khan, A., Du, D., Li, X. 2018. Lignin depolymerization and utilization by bacteria. Bioresour. Technol. 269, 557-566.

42. Yeom, S., Yeom, J., Park, W. 2010. NtrC-sensed nitrogen availability is important for oxidative stress defense in *Pseudomonas putida* KT2440. J Microbiol. 48(2), 153-9.

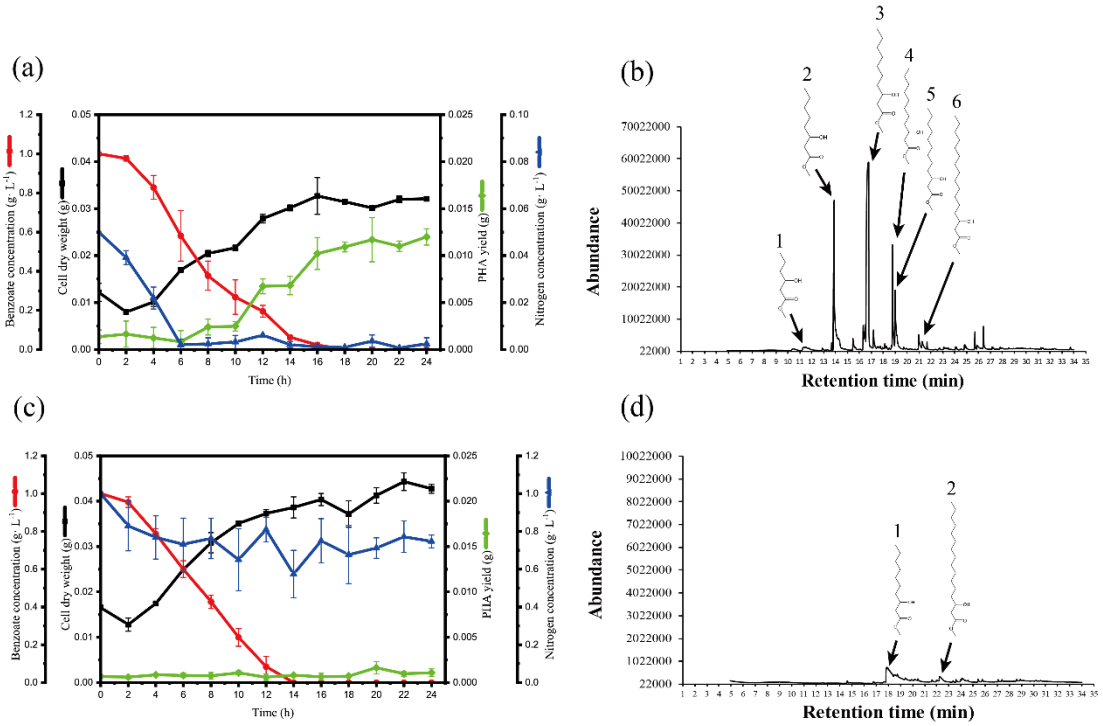

Figure 1. Time course of growth-associated PHA synthesize in *P. putida* KT2440 and GC/MS spectrum of PHA ester groups after the acidic methanolysis reaction under nitrogen limited (a), (b) or surplus conditions (c), (d).

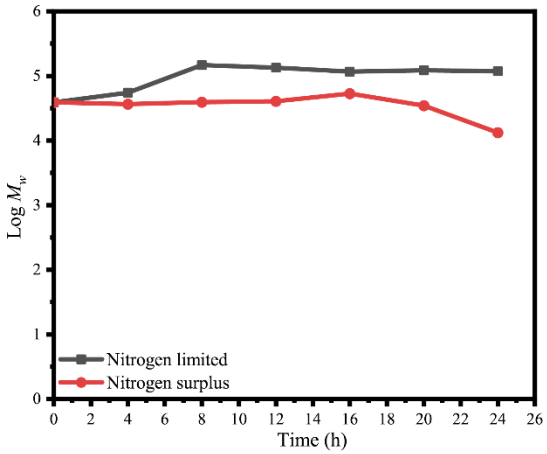

Figure 2. GPC results for the PHA from nitrogen-limited conditions and nitrogen-surplus condition.

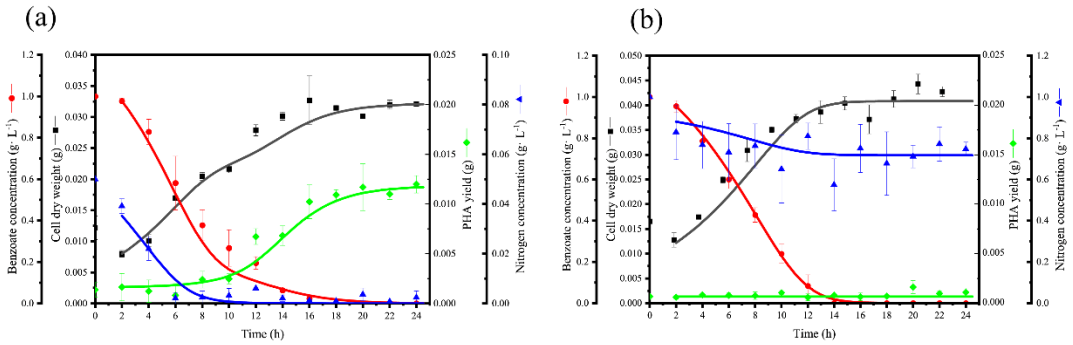

Figure 3. Kinetic modeling of *P. putida* KT2440 growth on benzoate with two nitrogen source conditions: nitrogen limited condition with 50 mg·L^{-1} ammonium chloride (a) nitrogen surplus condition with 1g·L^{-1} ammonium chloride (b).

Table 1. Characteristics of PHA monomers under nitrogen limited and surplus conditions at 24 hours of fermentation.

Nitrogen supply condition	No.	GC/MS characterization	PHA monomer	Molecular formula	Mol%
Nitrogen limited	1	Methyl 3-hydroxyhexanoate	3-hydroxyhexanoate (3HH)	$C_6H_{12}O_3$	6.27
	2	Methyl 3-hydroxyoctanoate	3-hydroxyoctanoate (3HO)	$C_8H_{16}O_3$	51.96
	3	Methyl 3-hydroxydecanoate	3-hydroxydecanoate (3HD)	$C_{10}H_{20}O_3$	28.08
	4	Methyl 3-hydroxyundecanoate	3-hydroxyundecanoate (3HUD)	$C_{11}H_{22}O_3$	8.54
	5	Methyl 3-hydroxydodecanoate	3-hydroxydodecanoate (3HDD)	$C_{12}H_{24}O_3$	4.82
	6	Methyl 3-hydroxyhexadecanoate	3-hydroxyhexadecanoate (3HHD)	$C_{16}H_{32}O_3$	0.34
Nitrogen surplus	1	Methyl 3-hydroxydecanoate	3-hydroxydecanoate (3HD)	$C_{10}H_{20}O_3$	58
	2	Methyl 3-hydroxyhexadecanoate	3-hydroxyhexadecanoate (3HHD)	$C_{16}H_{32}O_3$	42

Research Highlights

- Benzoate-to-PHA conversion by *P. putida* KT2440 was demonstrated for the first time.
- Nitrogen supply condition acted as the trigger of the synthesis of PHA monomers.
- Two distinct PHA synthesis patterns were revealed by kinetic modeling.
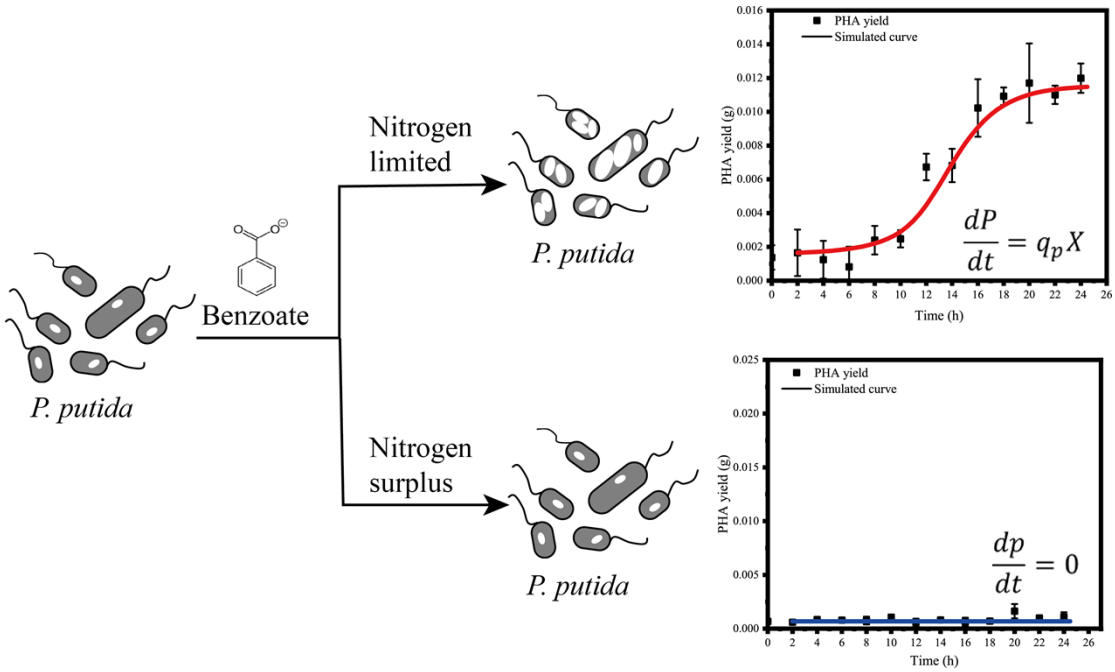
Graphical abstract